KSME

Springer

Journal of Mechanical Science and Technology 37 (9) 2023

Original Article
DOI 10.1007/s12206-023-0805-y

Keywords:
· Coherence analysis through continuous cross wavelet transform
· Electromagnetic noise
· Medium and low speed maglev train
· Sound source identification

Correspondence to:
Chunjun Chen
cjchen@swjtu.edu.cn

Citation:
Chen, C., Ou, F., Liao, X., Deng, J. (2023). Research on characteristic frequency extraction and sound source identification of electromagnetic noise of medium and low speed maglev train. Journal of Mechanical Science and Technology 37 (9) (2023) 4467~4476.
http://doi.org/10.1007/s12206-023-0805-y

Received January 9th, 2023
Revised April 19th, 2023
Accepted June 8th, 2023

† Recommended by Editor No-cheol Park

Research on characteristic frequency extraction and sound source identification of electromagnetic noise of medium and low speed maglev train

Chunjun Chen[1,2], Fengyu Ou[1], Xiaokang Liao[3] and Ji Deng[1]

[1]School of Mechanical Engineering, Southwest Jiaotong University (SWJTU), Chengdu 610031, China, [2]Technology and Equipment of Rail Transit Operation and Maintenance Key Laboratory of Sichuan Province, Southwest Jiaotong University (SWJTU), Chengdu 610031, China, [3]School of Mechanical Engineering, Xihua University (XHU), Chengdu 610039, China

Abstract For the operational noise of a medium-low speed maglev train, this paper proposes a method to achieve sound source identification based on characteristic frequency extraction and coherence analysis through continuous cross wavelet transform. Field tests were conducted on a main line in China on the operational noise, vibration and traction current of linear induction motor in the medium-low speed maglev train. The proposed method was applied to the test data to analyze the operational noise properties. The characteristic frequencies were extracted from all the three test target signals for coherence analysis through continuous cross wavelet transform, which verifies the transmission characteristics of electromagnetic noise. The coherence spectrum of noise-vibration signal and current-vibration signal showed that the operational noise in the starting and braking stages mainly originates from the high-frequency vibration excited by the high-frequency harmonics in the traction current of the traction motor.

1. Introduction

Although rail transit is convenient for people's travel during its development, passengers in the meanwhile put forward higher requirements for riding comfort. Among all the unpleasant factors, vibration noise is the most noticeable disturbance during the ride process. If the vibration level of the train is too high, besides the riding comfort, it may affect the structural safety and reliability of the train by the possible structural damage to the train parts. In addition, the high-intensity interior noise will bring negative emotions, such as depression and irritation, to passengers, drivers and crews, threaten the driving safety, and affect the life quality of residents around the train line.

Numerous researches have been conducted on rail transit noise. Choi [1] tested and analyzed the interior noise of the Korean KTX train running in tunnels with different track types, concluding that the increase of interior noise on the slab track at the same speed was greater than that on the ballast track. Wang et al. [2] discussed the relationship between noise exposure level and noise annoyance. If the noise exposure level exceeds 79 dB, it may cause serious annoyance to passengers. To study the noise problem caused by the elevated rail transit in Beijing, Nie et al. [3] carried out the noise field test on the elevated section of Beijing Metro Line 5. The impact of the train's operational noise on the steel box girder section of an elevated bridge is greater than that on the reinforced concrete box girder section. Zhang et al. [4] used the coupled vibration theory of vehicle-rail-bridge and the boundary element method to calculate the radiated noise of vibrating bridges. They conducted research on a simple-supported concrete U-beam used in Chongqing Metro Line 1. Lyu [5] established a noise prediction model capable of predicting rail transit noise and proposed effective methods to reduce noise. Jang et

al. [6] compared the internal noise reduction performance of each section in a Korean KTX train by multi-channel active noise control technique. Noh et al. [7] conducted research on resolution improvement to identify low-frequency noise sources in the high-speed train. That method was verified by tests and applied to high-speed train.

According to the type of vibration source, the noise sources of rail vehicles are mainly classified as (1) mechanical noise caused by wheel-rail contact, (2) electromagnetic noise of the traction system, and (3) aerodynamic noise of the car body structure [8, 9]. Different from rail transit vehicles with wheel-rail contact, medium-low speed maglev trains are driven by electromagnetic levitation and linear motors, so the mechanical noise caused by wheel-rail contact and gearbox transmission can be ignored. In addition, the running speed of medium-low speed maglev train is generally within 100 km/h, and the operational noise is mainly generated in the starting and braking stages in which the running speed is low. Nevertheless, aerodynamic noise can only take the dominant position when the running speed is higher than 250 km/h [10], which is suitable for high-speed train study. Therefore, in theory, the electromagnetic noise of the traction system is supposed to be the main source of operational noise for the medium-low speed maglev train, which is predominantly responsible for the overall noise sound pressure level at the vehicle bottom, but difficult to control and eliminate due to its complex components and high frequency.

The harsh high-frequency noise emitted by motors is usually the electromagnetic noise, which draws special attention of motor designers. Various control methods in variable speed motors are one of the factors that affect the motor noise and vibration. Wallace [11] found that non-sinusoidal current excitation is the noise source of variable speed motors by studying the vibration and noise of induction motors, permanent magnet motors and switched reluctance motors. When the input current contains harmonics, high-frequency harmonics will cause electromagnetic vibration and noise in motors. Belmans [12] carried out research on the relationship between frequency converter and motor vibration and noise. After analyzing the electromagnetic force spectrum of motor vibration powered by frequency converter, and calculating the motor stator structure modal, Belmans compared the frequency of electromagnetic force and stator modal to discover their relationship and conducted tests in induction motor to verify the findings. Mikhail et al. [13] comprehensively analyzed the source of vibration in the induction motor under the control of variable frequency driver and proposed suggestions on preventing VFD motor from excessive vibration. Jang et al. [14] proposed a method of predicting the vibration caused by electromagnetic force from other types of vibration occurring in the motor. They put a 9-slot 8-pole permanent magnet synchronous motor as an example and illustrated its electromagnetic vibration characteristics. The validity of the method was confirmed by comparing the motor vibration velocity with the velocity obtained from electromagnetic vibration coupling analysis. Lu et al. [15] suggested a hybrid evaluation method of electromagnetic force and vibration taking high-frequency current harmonics caused by inverter into consideration. Applied to the internal permanent motor, this method can significantly reduce computational burden with the commonly used finite element method, in contrast to the multi-physical program.

In recent years, many studies have been carried out on the interior noise of high-speed trains and urban subways, but the study on the noise of medium-low speed maglev train is still a blank field. However, the noise problem actually exists in medium and low speed maglev trains [16], and the noise source mechanism is not the same as that of wheel-rail noise. Aiming at the problem of high-frequency electromagnetic noise during the operation of medium-low speed maglev train, this paper studied the sound source identification based on the extraction of signal characteristic frequency and the coherence analysis through continuous cross-wavelet transform, and employed Hilbert transform to demodulate the modulation phenomena in the signal. The validity of this paper was confirmed by tests and analysis on the operational noise, vibration and traction current of linear induction motor in the medium-low speed maglev train on a main line in China. This research can provide a theoretical and practical basis for vibration and noise reduction from the perspective of excitation source.

2. Basic theories

2.1 Wavelet denoising

The basic idea of wavelet denoising is to obtain the wavelet coefficient of the raw signal by wavelet transform. After decomposed by wavelet, the wavelet coefficient of signal is large, while the wavelet coefficient of noise is small, smaller than that of the signal. By selecting an appropriate threshold, the wavelet coefficient greater than the threshold is considered to be generated by signal and should be retained. Instead, the wavelet coefficient less than the threshold is considered to be generated by noise, and should be eliminated to achieve noise filtering [17].

From the perspective of signal processing, wavelet denoising is similar and superior to band-pass filtering (BPF), since after wavelet denoising the signal can greatly retain the characteristics of the original signal. Therefore, wavelet denoising can be regarded as a synthesis of feature extraction and BPF. The main processes of wavelet denoising are shown in Fig. 1.

The mathematical model of a raw signal with noise can be stated as:

$$T(k) = f(k) + \varepsilon \cdot e(k) \quad k = 0, 1, 2, \ldots, n-1 \tag{1}$$

where $T(k)$ is raw signal with noise, $f(k)$ is useful signal, $e(k)$ is noise and ε is the standard deviation of noise figure.

Assuming that $e(k)$ is Gaussian white noise, the useful signal is usually low-frequency or relatively stable, while the noise signal is high-frequency. When the $T(k)$ signal is decomposed

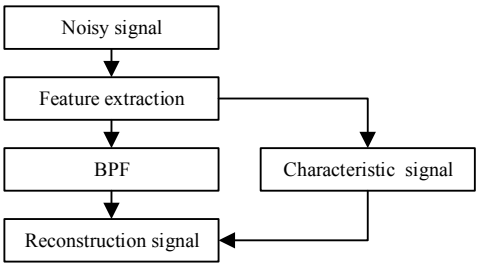

Fig. 1. Wavelet denoising processes.

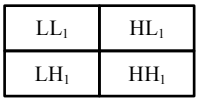

Fig. 2. Wavelet decomposition of raw signal.

by wavelet, it can be divided into four parts: LL_1, HL_1, LH_1, and HH_1, and noise is usually included in HL_1, LH_1 and HH_1, as shown in Fig. 2. Noise cancellation can be easily realized after filtering the corresponding wavelet coefficients of HL_1, LL_1 and HH_1, and reconstructing the raw signal.

The selection of threshold in noise filtering is based on the idea of minimax approximation. Under the constraint condition that the processed signal is maximum approximate to the original signal, a soft threshold is selected and employed in the wavelet coefficient process. This method can reinforce noise filtering and improve the signal-to-noise ratio.

2.2 Hilbert transform demodulation

For signal $x(t)$ in the time domain, after Hilbert transform, $H[x(t)]$ can be stated as [18]:

$$\mathrm{H}\left[x(t)\right]=\tilde{x}(t)=\frac{1}{\pi}\int_{-\infty}^{+\infty}\frac{x(\tau)}{t-\tau}d\tau\,. \tag{2}$$

According to Eq. (2), $H[x(t)]$ is the result of convolving the signal $x(t)$ with $1/\pi t$, that is, the response generated by the input signal $x(t)$ passing through a linear, time-invariant system with an impulse response of $1/\pi t$.

The Hilbert transform possesses linear superposition. For any scalars a_1 and a_2 and signals $x_1(t)$ and $x_2(t)$, $\mathrm{H}[x_1(t)+x_2(t)] = a_1\mathrm{H}[x_1(t)]+a_2\mathrm{H}[x_2(t)]$. The Hilbert transform of a constant is zero. The Hilbert transform of a sinusoidal signal $\sin(t)$ is $-\cos(t)$ and the Hilbert transform of a cosine signal $\cos(t)$ is $-\sin(t)$. $x(t)$ and $\tilde{x}(t)$ are different only in the phase spectrum, while identical in the amplitude spectrum, energy spectrum, and power spectrum. $-x(t)$ can be obtained after twice Hilbert transform of the signal $x(t)$. The signal $x(t)$ is orthogonal to its Hilbert transform, that is [19], $\int_{-\infty}^{+\infty}x(t)\tilde{x}(t)=0$.

If the signal $x(t)$ is the product of the slowly-varying signal $s(t)$ and the fast-varying signal $f(t)$, that is, $x(t) = s(t)f(t)$, an amplitude modulated signal is formed. To avoid overmodulation, set $s(t) \geq 0$. $Y(t)$ can be assumed as:

$$Y(t)=x^2(t)+\mathrm{H}^2\left[x(t)\right]. \tag{3}$$

Based on the Bedrosian product theorem, $H[x(t)]$ can be stated as [20]:

$$\mathrm{H}\left[x(t)\right]=\mathrm{H}\left[s(t)f(t)\right]=s(t)\mathrm{H}\left[f(t)\right]. \tag{4}$$

Simultaneous equations of Eqs. (3) and (4) can be stated as:

$$Y(t)=s^2(t)\left\{f^2(t)+\mathrm{H}^2\left[x(t)\right]\right\}. \tag{5}$$

$z(t)$ can be assumed as:

$$z(t)=f^2(t)+\mathrm{H}^2\left[x(t)\right]. \tag{6}$$

It is clear that $z(t) \geq 0$ and thus direct current components must be contained. It is assumed that $f(t)$ is the sum of the two harmonic signals:

$$f(t)=a_1\cos\omega_1 t+a_2\cos\omega_2 t\,. \tag{7}$$

After Hilbert transform, Eq. (7) can be stated as:

$$\mathrm{H}[f(t)]=a_1\sin\omega_1 t+a_2\sin\omega_2 t\,. \tag{8}$$

Substitute Eqs. (7) and (8) into Eq. (6):

$$z(t)=a_1^2+a_2^2+2a_1a_2\cos(\omega_1-\omega_2)t\,. \tag{9}$$

Eq. (9) shows that $z(t)$ consists of two parts, the square sum of the amplitudes of the two harmonics and the difference frequency component of the two harmonics. Substitute Eqs. (5)-(9):

$$Y(t)=s^2(t)(a_1^2+a_2^2)+2a_1a_2s^2(t)\cos(\omega_1-\omega_2)t\,. \tag{10}$$

If $s_A(t)$ and $f_A(t)$ can be assumed as:

$$s_A(t)=s^2(t)(a_1^2+a_2^2) \tag{11}$$

$$f_A(t)=2a_1a_2s^2(t)\cos(\omega_1-\omega_2)t\,. \tag{12}$$

$Y(t)$ can be stated as:

$$Y(t)=s_A(t)+f_A(t)\,. \tag{13}$$

ω_{max} is assumed as the highest frequency component of $s(t)$. If ω_1-ω_2 >> $2\omega_{max}$, an appropriate cut-off frequency ω_c can be selected from $s_A(t)$ and $f_A(t)$ through Hilbert LPF. Then the slowly-varying envelope $A(t)$ can be estimated from the slowly

-varying component $s_A(t)$ which is extracted from ω_c:

$$A(t)=\sqrt{s_A(t)}=\sqrt{a_1^2+a_2^2}s(t). \tag{14}$$

In Eq. (14), the slowly varying envelope only differs from the original envelope in amplitude.

2.3 Continuous cross-wavelet transform

Cross-wavelet is often used to detect coherence among signals, which can establish connections between different signals in the time-frequency domain [21]. Wavelet transform of signal $x(t)$ in the time domain can be stated as:

$$W_x(a,b)=\frac{1}{\sqrt{a}}\int_{-\infty}^{+\infty}x(t)\Psi^*(\frac{t-b}{a})dt \tag{15}$$

$$\Psi(t)=\pi^{-1/4}(e^{-j\alpha_0 t}-e^{-\alpha_0^2/2})e^{-t^2/2}. \tag{16}$$

In Eq. (15), *a* and *b* are scaling factor and translation factor, respectively, and * is complex conjugation. In Eq. (16), $\Psi(t)$ is Morlet mother wavelet function, and α_0 is the initial phase of wavelet transform. Cross-wavelet transform of signal $x(t)$ and $y(t)$ in the time domain, and the corresponding cross-wavelet coherence spectrum amplitude can be stated as:

$$W_{xy}(a,b)=W_x^*(a,b)W_y(a,b) \tag{17}$$

$$X_x(a,b)=W_{xy}^*(a,b)W_{xy}(a,b)=\left|W_{xy}(a,b)\right|^2. \tag{18}$$

In Eq. (18), the coherence between the two signals is positively correlated with $X_x(a, b)$, and $0 \le X_x(a, b) \le 1$.

3. Transmission and identification of electromagnetic noise sources

3.1 Transmission of electromagnetic noise sources

For railway traction, both locomotives and multiple units require the corresponding traction performance, such as smooth starting with sufficient traction, superior speed regulation performance, and high utilization rate during high-speed driving. The traction system should meet power or regenerative braking needs, while avoid idling or sliding situations as much as possible. To guarantee the performance above, the speed control system plays a particularly crucial role in a motor. The most commonly used speed regulation method for asynchronous induction motors is variable voltage variable frequency (VVVF) speed regulation. The medium and low speed maglev trains are powered by the third rail whose voltage and frequency are basically constant (The power frequency is 50Hz, and the line voltage is 1500 V.), and equipped with a specialized VVVF device, the traction converter. This device first converts three-phase AC with constant voltage and frequency into DC through a rectifier, and then converts DC into VVVF three-phase AC through an inverter. As an extremely important component of the traction control system for medium and low speed maglev trains, the traction inverter outputs VVVF three-phase AC to control the speed and torque of the linear induction motor. However, when the pulse width modulator (PWM) operates at a fixed switching frequency, due to the inductive load on the primary coil of the motor, the output current is not a smooth sinusoidal wave, but contains a large amount of high-frequency harmonic components. Meanwhile, the switching frequency of the controller determines the smoothness of the output current. When the power switching device contains more pulses within a cycle, it will generate higher switching frequency and fewer high-frequency harmonics, so that the current smoothness will be better. Relevant theories and experimental research show that the frequency component of high-frequency current harmonics is related to the inverter switching frequency and its multiple frequencies. Additionally, the traction current is not an ideal sinusoidal signal, but a superposition of fundamental and harmonic waves. Its high-frequency current harmonic components can bring high-frequency harmonics into the air-gap magnetic field, exciting high-frequency pulsating electromagnetic force, which will cause high-frequency vibration in the traction motor. The frequency components of the vibration and noise signals caused by the high-frequency current harmonic components are also mainly concentrated at the switching frequency and its multiple frequencies.

Medium and low speed maglev train adopts linear induction motor as traction motor, and is powered by frequency conversion power supply of traction inverter. In terms of performance, it pursues high power density, high thrust density, lightweight, miniaturization and wide speed regulation range, which results in large amplitude of high-frequency harmonics in the traction current. The harmonics will significantly affect the amplitude and frequency of electromagnetic force in the air gap magnetic field of motor, causing high-frequency electromagnetic exciting force. If the frequency of these electromagnetic exciting forces is equal or close to the inherent modal frequency of motor structure, high-frequency resonance will happen in the motor structure, which will amplify vibration and noise. Transmission

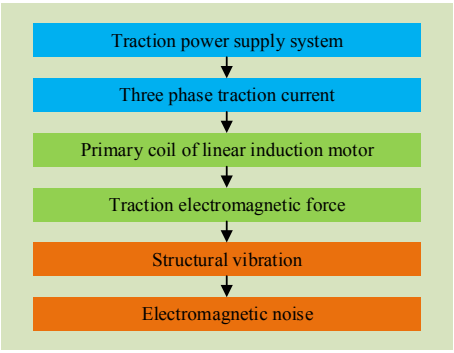

Fig. 3. Excitation and transmission of electromagnetic noise sources.

of vibration and noise in the medium and low speed maglev train is shown in Fig. 3.

3.2 Identification of electromagnetic noise sources

The noise, vibration and current signals collected in the test are preprocessed by wavelet denoising to remove the non-useful signals, so as to enhance the characteristic frequency of vibration and electromagnetic noise in the medium and low speed maglev train. Then the time-domain signals in the whole running operation are processed by short-time Fourier transform (STFT), to find the main stage of noise with large time-domain signals and its corresponding dominant frequency range. Next, the noise, vibration and current signals are processed by fast Fourier transform (FFT) to obtain their characteristic frequency components. Since the signals may be modulated in the frequency domain, if modulation occurs, the signals should be demodulated by Hilbert transform (HT), and processed by FFT to obtain the spectrum in which demonstrates the main characteristic frequency components of the three signals. Finally, the three signals are processed by continuous cross wavelet transform for the time-frequency coherence, which can identify the source of noise. Fig. 4 shows the processes of electromagnetic noise characteristics and sound source identification in the medium and low speed maglev train based on characteristic frequency extraction and coherence analysis through continuous cross wavelet, including three steps:

1) **Signal preprocessing:** The input signals are preprocessed by wavelet denoising. Since the wavelet coefficients of different frequency components in the signal reflect different properties at different screening scales, the noisy signals are wavelet filtered to reduce the wavelet coefficients generated by noise and preserve those generated by the real signal.
2) **Signal characteristic frequency extraction:** The original noise signal changes with the running speed of the train in the time domain, and the electromagnetic noise signal is generally concentrated in the starting and braking stages during the operation of the medium and low speed maglev train. Hence, the noise signal should be analyzed in the time domain to determine the stage of the largest noise emission. Then through STFT the noise, vibration and current signals are processed at the same time to obtain the frequency variation range and the approximate main frequency components of noise during the operation. The characteristic frequency of the signal can be obtained from the time-domain range with large electromagnetic noise processed by FFT. Since the main frequency components of electromagnetic noise are mainly concentrated in the high-frequency stage and the high frequency components tend to be modulated, if modulation occurs, the signals should be demodulated by HT and processed by FFT to obtain the spectrum. The characteristic frequency of each signal can be extracted from the spectrum to show the frequency-domain characteristics of electromagnetic noise for noise source identification in the frequency domain.
3) **Continuous cross wavelet coherence analysis:** The method above only compares the characteristic frequency in the spectrum of a section with large noise and obvious main frequency during the whole operation for characteristic frequency identification. To further study the coherence among noise, traction motor vibration and current signals during the whole operation, continuous cross wavelet transform is employed to establish the correlation among signals in the time-frequency domain. This method can clearly demonstrate the acoustic-vibration-electromagnetic coupling characteristics of the medium and low speed maglev train during the whole operation process.

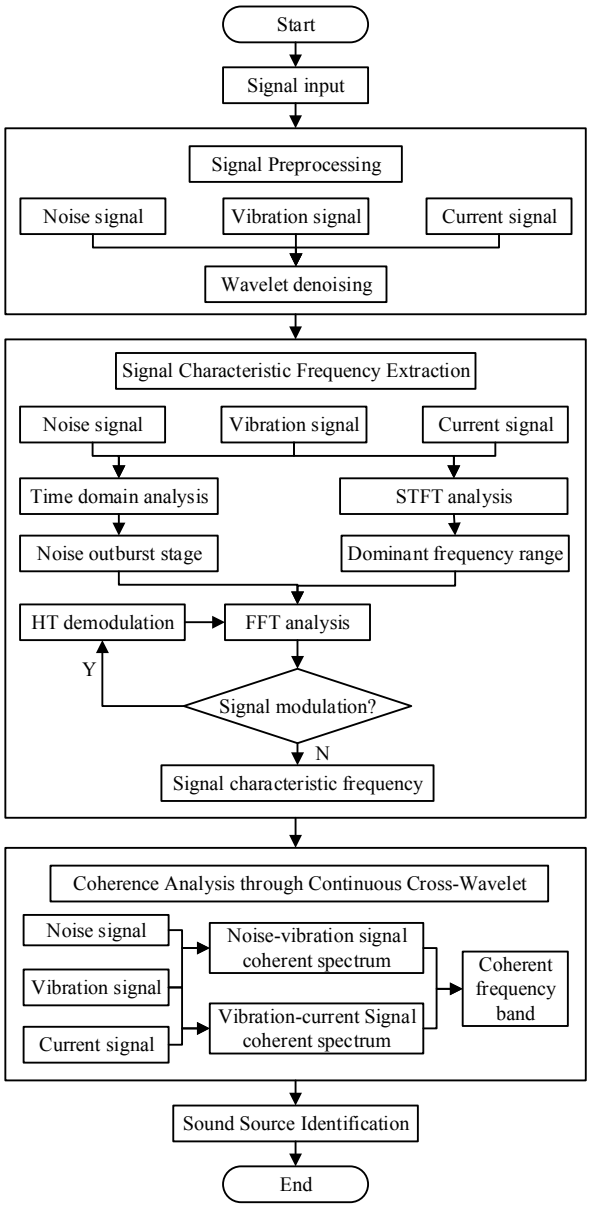

Fig. 4. Electromagnetic noise characteristics and sound source identification processes in the medium and low speed maglev train.

4. Experimental research

To verify the validity of the theories and methods above, relevant tests were carried out in the medium and low speed maglev trains on a demonstration line in China. This paper tested the underbody noise sound pressure, vibration acceleration of linear traction motor in three directions, and primary coil three-phase traction current of linear traction motor. The experimental methods conform to the Chinese national standard GB 14892-2006 [22] and the international standard ISO 14837-1-2005 [23].

Fig. 5 shows the layout of sensors and measuring points on the underbody. To measure the sound field distribution characteristics of the whole vehicle, ten linear induction motors are set and marked from M1 to M10 in a train, and the middle of each motor is selected as the noise measuring point. M1 and M2 in the end, and M5 and M6 in the middle are selected as the measuring points to test the three-phase input current and the original current of the linear traction motors, as well as the vibration acceleration of the linear traction motors in three directions. Since the current harmonics is mainly caused by the traction power supply system, M1 and M2 are set close to the traction inverter and the input current is not used by the electric appliance, which can well reflect the characteristics and performance of the variable frequency speed regulation system. M5 and M6 are located in the middle of the motor to generally reflect the input current characteristics of motors in the whole vehicle.

Fig. 6 demonstrates the sensor installation. Current sensors are installed at the current input end of the linear traction motor to measure the input current. The connections between the suspension frame and the linear motor are selected as vibration acceleration measuring points, and install the three-direction acceleration sensors which are positioned with the tooling. The direction of the three-direction acceleration sensor is consistent with the vehicle coordinate system, in which X represents the longitudinal direction, Y represents the transverse direction, and Z represents the vertical direction. Noise sensors are installed right above the motor whose microphones are directly facing the coil of the traction motor to measure the sound pressure distribution of the noise from the linear motor and the whole vehicle underbody.

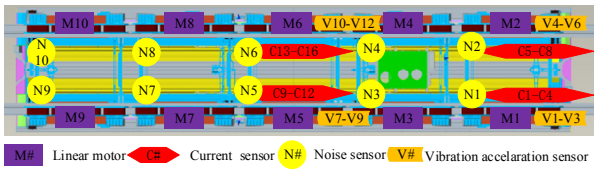

Fig. 5. Arrangement of underbody sensors and measuring points in a medium and low speed maglev train.

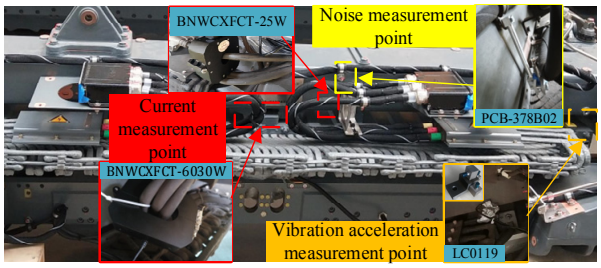

Fig. 6. Field installation layout of sensors.

Field tests were conducted to measure the dynamic operation of the train at three test speeds, 20 km/h, 40 km/h and 60 km/h. The train was loaded in AW0 mode. During the test, the train was first statically suspended. Then as the primary of linear traction motor was energized, the train was propelled by the traction system to accelerate to each test speed. At each test speed, the train operated at a constant speed for the same time and decelerated to brake at the end of the test. Underbody noise sound pressure, vibration acceleration of traction motor and three-phase traction current were measured, respectively, at the three test speeds, and each test speed was tested three times. The sampling frequency of all sensors used in the actual test was 50 kHz, which is sufficient to guarantee the accuracy of transient signals of vibration acceleration, traction current and noise.

4.1 Noise signal analysis in the time domain

The analysis of the raw sound pressure signal is not clear and unable to reflect the perception of sound by human ear. Therefore, the raw sound pressure signal should be converted

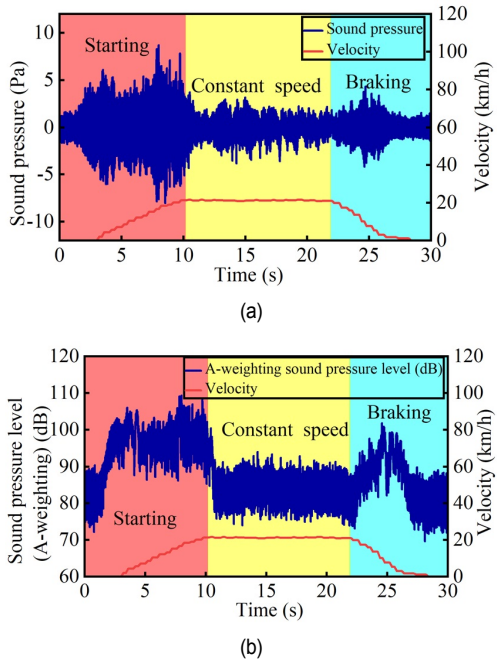

Fig. 7. Time-domain curve of noise sound pressure and A-weighting sound pressure level varying with the train running speed: (a) sound pressure; (b) A-weighting sound pressure level.

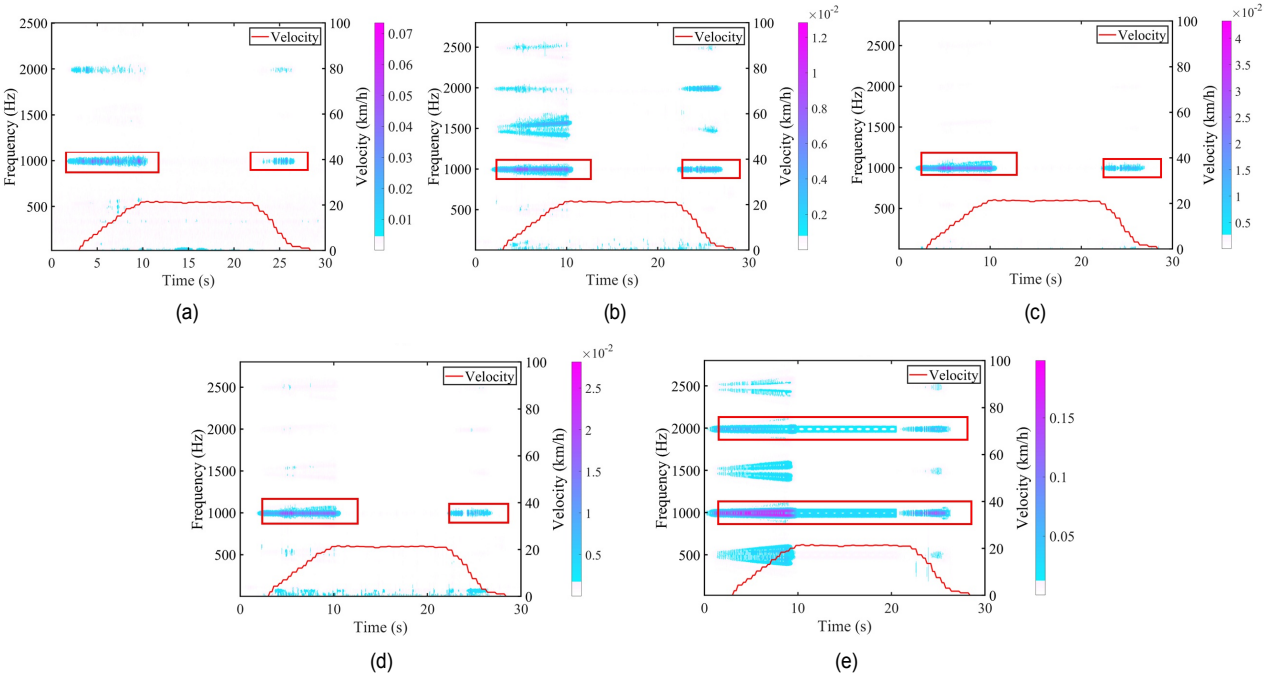

Fig. 8. Time-frequency analysis of noise, vibration and current signals: (a) sound pressure; (b) lateral vibration acceleration; (c) longitudinal vibration acceleration; (d) vertical vibration acceleration; (e) traction current.

to sound pressure level and A-weighted for better evaluation.

Fig. 7 demonstrates the curve of noise sound pressure and A-weighted sound pressure level varying with the train running speed. The noise sound pressure and A-weighting sound pressure level at the starting stage are significantly higher than those at the constant speed and braking stages, which is consistent with the characteristics of electromagnetic noise. During the starting and braking stages, the linear traction motor needs to provide large traction force, resulting in large amplitude of high-frequency harmonic components in the traction current, which will cause noise amplification. Therefore, this paper focused on the analysis of the starting stage.

4.2 Time-frequency analysis with STFT and characteristic frequency extraction of noise, vibration and current signals

Sec. 4.1 analyzed the intensity of the noise signal in the time domain. To identify the sound source and extract the characteristic frequency, Sec. 4.1 explored the frequency components that increase the noise amplitude, and the frequency-domain characteristics of the noise, vibration and current signals. Sec. 4.2 applied STFT to processing the noise, vibration and current signals, and analyzed the frequency components contained in the noise signal at different stages.

Fig. 8 illustrates the time-frequency analysis with STFT of noise, vibration and current signals. The research on the current signal only focuses on the high-frequency harmonic components, for the low-frequency components adjacent to the fundamental frequency were filtered. In Fig. 8(a), the noise sound pressure signal contains the noticeable frequency components of about 1000 Hz during the starting and braking stages, which indicates that the operational noise amplification in the same stages is mainly related to the increase of noise at the frequency about 1000 Hz. From Figs. 8(b)-(e), both the vibration acceleration in three directions and traction current of the linear induction motor possess the obvious high-frequency components of about 1000 Hz, which are mainly concentrated in the starting and braking stages. It shows that the high-frequency operational noise signal comes from the high-frequency vibration of the traction motor. Electromagnetic noise is responsible for the noise amplification whose characteristic frequencies are mainly at the frequency of about 1000 Hz.

To further explore the characteristic frequency of each signal, the noise, vibration and current signals at the starting stage were processed by FFT to obtain the corresponding spectra and inspected for modulation. Fig. 9 shows the spectrum of noise, vibration and current signals during the starting phase. In Figs. 9(a), (d), (e) and (f), both the operational noise and the three-direction vibration of the linear induction motor possess the characteristic frequency 994.33 Hz and some main harmonic components, such as 497.33 Hz and 1998.65 Hz, among which 497.33 Hz, 994.33 Hz and 1998.65 Hz have the relation of frequency multiplication. 1998.65 Hz is four times and 994.33 Hz is two times of 497.33 Hz. Fig. 9(b) shows the spectrum of the high-frequency harmonics in the current signal. The high-frequency current signal of 994.33 Hz is modulated with the current fundamental frequency of 21.66 Hz. Fig. 9(c) is obtained after demodulation by the Hilbert transform mentioned in Sec. 2 and then the FFT processes, which verifies the valid-

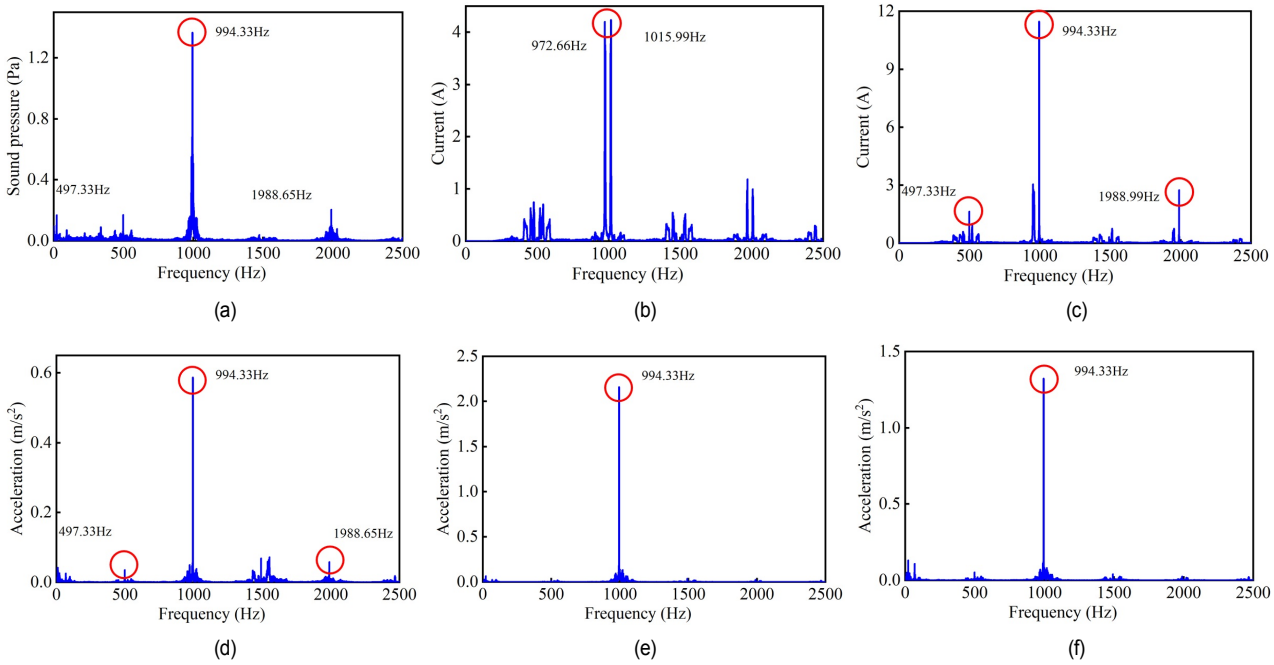

Fig. 9. Spectrum of noise, vibration and current signals: (a) sound pressure; (b) modulated current; (c) demodulated current; (d) lateral vibration acceleration; (e) longitudinal vibration acceleration; (f) vertical vibration acceleration.

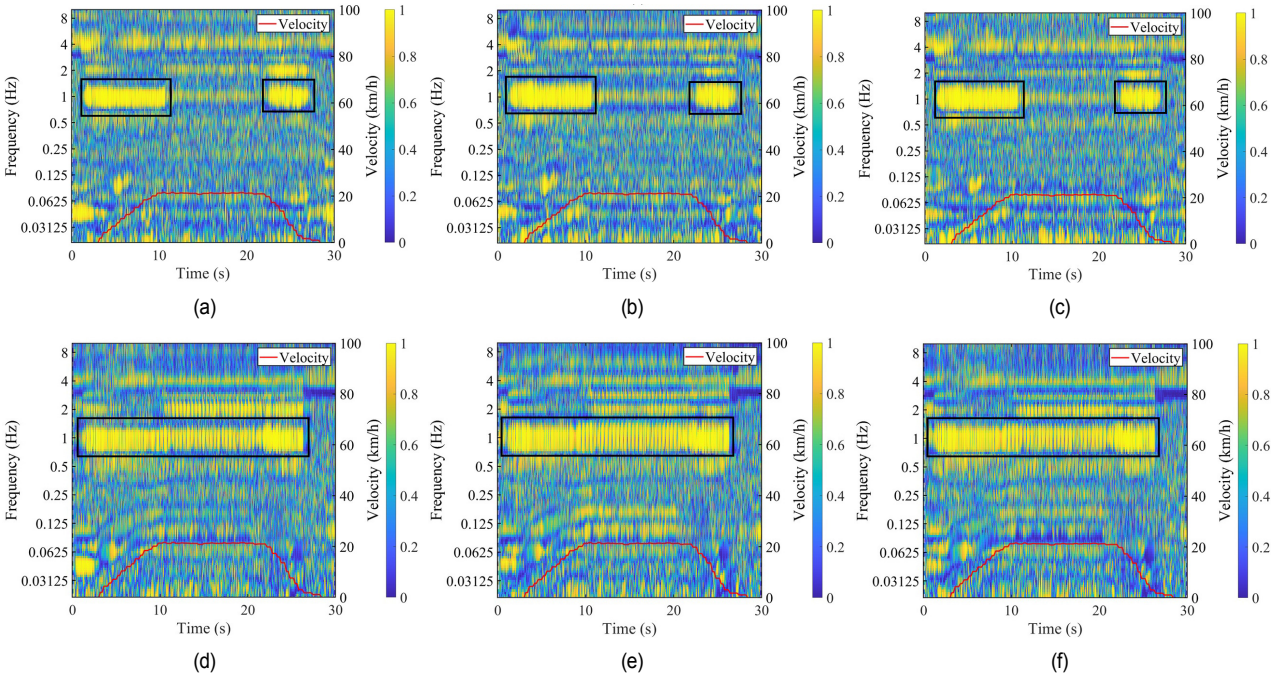

Fig. 10. Noise-vibration and current-vibration coherence spectrum through continuous cross wavelet transform: (a) noise-lateral vibration; (b) noise-longitudinal vibration; (c) noise-vertical vibration; (d) current-lateral vibration; (e) current-longitudinal vibration; (f) current-vertical vibration.

ity of the Hilbert demodulation. The characteristic frequency of 994.33 Hz illustrated in Fig. 9(c) is consistent with the characteristic frequency of noise and vibration signals, which indicates that the high-frequency motor vibration caused by the high-frequency current harmonics is the main reason for the noise amplification during the starting and braking phases in the medium and low speed maglev train operation, and also verifies the transmission characteristics of electromagnetic noise.

4.3 Coherence analysis through continuous cross-wavelet transform

Sec. 4.2 analyzed the noise, vibration and current signals in the frequency domain, and extracted the main frequency char-

acteristics of the signals.

From some modulated signals, useful characteristic frequencies are extracted by demodulation. To study the correlation between the electromagnetic vibration and noise during the whole operation of the medium and low speed maglev train, Sec. 4.3 obtained from the continuous cross wavelet transform the noise-vibration and the current-vibration coherence spectra as shown in Fig. 10. Figs. 10(a)-(c) demonstrate that the coherence frequency band of noise and vibration in the starting and braking stages is 1000 Hz. The frequency band of 2000 Hz~4000 Hz also shows a strong coherence. It is proved that the main source of the operational noise in the starting and braking stages is the high-frequency vibration of the linear induction motor. Due to the large amplitude of traction current in the starting and braking stages, the significant high-frequency motor vibration excited by the traction current plays a predominant role in the overall noise in the operation. However, in the constant speed stage, the traction current is small with subtle amplitude, so that the motor vibration only imposes light impact on the overall noise. Therefore, in the starting and braking stages, a strong coherence appears in the characteristic frequencies of the operational noise and the motor vibration signals, while in the constant speed stage, the coherence is weak for the noise produced by the motor vibration only takes a subordinate position in the overall vehicular noise.

Figs. 10(d)-(f) show that in the whole stage the coherence coefficients of current and vibration are high at 1000 Hz and relatively high during 2000 Hz~4000 Hz, which indicates that the high-frequency vibration of linear induction motor is mainly caused by the high-frequency harmonic components of traction current. Since the motor vibration is excited by the electromagnetic force whose frequency is consistent with that of the traction current, no matter how the traction current changes, a strong coherence will always exist in the characteristic frequencies of the motor vibration and the traction current signals. Hence a significant coherence is continuously displayed in the coherence spectrum at 1000 Hz and its multiple frequencies. The test verifies the validity of the signal coherence analysis.

5. Conclusions

In response to high-frequency electromagnetic noise during the operation of medium and low speed maglev trains, this paper carried out the research on sound source identification based on signal frequency-domain characteristics extraction and coherence analysis through continuous cross wavelet transform. Hilbert transform was employed to solve modulation. The method proposed in this paper was applied to field tests on a main line to measure noise, vibration and current signals for frequency-domain characteristics extraction and sound source identification with signal coherence. Aiming at the noise problem of the existing medium-low speed maglev train, which is different from that of the wheel-rail train, this research is helpful for the design of the train, especially for the reduction of high-frequency vibration and noise of the motor caused by current harmonics. Some conclusions can be drawn as follows:

1) Different from wheel-rail vehicles, the operational noise of medium and low speed maglev trains is mainly concentrated in the starting and braking stages, whose characteristic frequencies at the two stages are 994.33 Hz and the adjacent high-frequency components.
2) Through characteristic frequency extraction, the main frequency components of vibration and current signals are also 994.33 Hz, which indicates that the operational noise in the starting and braking stages of medium and low speed maglev train mainly originates from the high-frequency vibration of the traction motor. Hilbert transform was applied to the modulation of the current high-frequency components and its fundamental frequency for demodulation and ideal characteristic frequency extraction.
3) Coherence analysis through continuous cross-wavelet transform can accurately locate the coherent frequency bands between the operational noise and linear induction motor vibration as well as between linear induction motor vibration and traction current. The coherence spectrums can accurately identify the electromagnetic noise source, which verifies that the high-frequency vibration of motor is excited by the high-frequency harmonic components in the traction current.

Acknowledgments

This work was supported by the National Natural Science Foundation of China (No. 51975487, No. U2034210), China, Postdoctoral Science Foundation (No. 2022M722633), China, the Natural Science Foundation of Sichuan Province (No. 2022NSFSC1991, No. 2022NSFSC0395), China, and the Fundamental Research Funds for the Central Universities (No. 2682022CX011), China.

References

[1] S. Choi, Interior noise of Korean high-speed trains in tunnels, *Foreign Railway Vehicles*, 53 (2016) 15-18.
[2] S. Wang, W. Hu and R. Song, The management and assessment of environmental noise of urban rail transit system, *7th Advanced Forum on Transportation of China (AFTC 2011)* (2011) 208-210.
[3] N. Zhili and C. Yanmei, Experimental study of environmental noise induced by elevated rail transit of beijing metro line 5, *2010 International Conference on Mechanic Automation and Control Engineering* (2010) 1984-1987.
[4] Z. Xun, L. Xiaozhen and W. Guoqiang, Vibration and sound radiation of rail transit viaduct, *2011 International Conference on Electric Technology and Civil Engineering (ICETCE)* (2011) 937-940.
[5] J. Lyu, A prediction model of urban rail transit noise, *2020 International Conference on Communications, Information System and Computer Engineering (CISCE)* (2020) 137-142.
[6] H. Jang, Y. M. Kim and J. Chung, KTX's interior noise reduc-

tion performance comparison for each section using multichannel active noise control, *2012 12th International Conference on Control, Automation and Systems* (2012) 1265-1270.
[7] H. M. Noh and J. W. Choi, Identification of low-frequency noise sources in high-speed train via resolution improvement, *J. of Mechanical Science and Technology,* 29 (9) (2015) 3609-3615.
[8] Y. Moritoh, Y. Zenda and K. Nagakura, Noise control of high speed shinkansen, *J. of Sound and Vibration*, 193 (1996) 319-334.
[9] C. Mellet, F. Letourneaux and F. Poisson, High speed train noise emission: latest investigation of the aerodynamic/rolling noise contribution, *J. of Sound and Vibration*, 293 (2006) 535-546.
[10] S. G. Zhang, Noise mechanism, sound source localization and noise control of 350 km/h high-speed train, *China Railway Science*, 30 (1) (2009) 86-90.
[11] A. K. Wallace, R. Spee and L. G. Martin, Current harmonics and acoustic noise in ac adjustable-speed drives, *IEEE Transactions on Industry Applications*, 26 (1990) 267-273.
[12] R. J. M. Belmans, D. Verdyck and W. Geysen, Electromechanical analysis of the audible noise of an inverter-fed squirrel-cage induction-motor, *IEEE Transactions on Industry Applications*, 27 (1991) 539-544.
[13] M. Tsypkin, Vibration of induction motors operating with variable frequency drives — A practical experience, *2014 IEEE 28th Convention of Electrical and Electronics Engineers in Israel (IEEEI)* (2014) 1-5.
[14] I. S. Jang, S. H. Ham and W. H. Kim, Method for analyzing vibrations due to electromagnetic force in electric motors, *IEEE Transaction on Magnetic*, 50 (2) (2014) 297-300.
[15] Y. Lu, J. Li and K. Yang, A hybrid calculation method of electromagnetic vibration for electrical machines considering high-frequency current harmonics, *IEEE Transaction on Industrial Electronics*, 69 (10) (2022) 10385-10395.
[16] F. Ou, X. Liao, C. Yi and J. Lin, Field measurements and analyses of traction motor noise of medium and low speed maglev train, *Energies*, 15 (23) (2022) 9061.
[17] W.-S. Ma, X.-P. Ren and Z.-B. Chen, A new signal analysis method after wavelet packet de-noising, *2008 International Conference on Wavelet Analysis and Pattern Recognition* (2008) 426-431.
[18] S. L. Hahn, *Hilbert Transform in Signal Processing*, Artech House, USA (1996).
[19] M. Feldman, Hilbert transform in vibration analysis, *Mechanical Systems and Systems Processing*, 25 (2011) 735-802.
[20] E. Bedrosian, A product theorem for hilbert transform, *Proceedings of the IEEE*, 51 (1963) 868-869.
[21] J.-G. Shen and D.-Y. Yuan, The properties of biorthogonal bivariate wavelet packets, *2007 International Conference on Wavelet Analysis and Pattern Recognition* (2007) 1608-1612.
[22] GB 14892-2006, *Noise Limit and Measurement for Train of Urban Rail Transit*, China National Standardization Administration (2006).
[23] ISO 14837-1-2005, *Mechanical Vibration - Ground-Borne Noise and Vibration Arising from Rail System - Part 1: General Guidance*, ISO (2005).

Chunjun Chen received the Ph.D. from Southwest Jiaotong University in 2006 and the M.A. from University of Electronic Science and Technology of China in 1993. He is a Professor of Mechanical Engineering, Southwest Jiaotong University, director of Department of Measurement and Control and Mechano-electronic Measurement and Control Laboratorial Center and Deputy Director of the Technology and Equipment of Rail Transit Operation and Maintenance Key Laboratory of Sichuan Province. His interests are in the area of vibration, noise and aerodynamics of high-speed trains, traffic equipment, electromechanical systems, advanced control and measurement theory, electromechanical control and measurement system.

Fengyu Ou received the B.S. in Mechanical and Electronic engineering from China University of Petroleum (East China) in 2020. He is currently a postgraduate student in Mechanical Engineering, Southwest Jiaotong University, Sichuan, China. His research interests include mechatronics, control and measurement and medium-low speed maglev train.

Xiaokang Liao received the B.S. from Wuhan Polytechnic University in 2015, M.S. in Mechanical Engineering, Southwest Jiaotong University in 2018, Ph.D. from the Laboratory of Traction Power of Southwest Jiaotong University in 2022. Now he is a lecturer in Mechanical Engineering, Xihua University.

Ji Deng received the B.E. from the School of Instrument Science and Opto-electronics Engineering from Hefei University of Technology, Hefei, China, in 2014, and the Ph.D. from the School of Precision Instrument and Opto-Electronics Engineering from Tianjin University, Tianjin, China, in 2021. He is currently an Assistant Professor of Mechanical Engineering, Southwest Jiaotong University, Chengdu, China. His research interests include rail transit smart operation & maintenance, 3D sensing and related applications.